in (*9*, *10*). The single-layer lithographic fabrication of the metalenses can make use of existing foundry technology (deep-UV steppers) used in the manufacturing of integrated circuits, which is crucial for high throughput.

## REFERENCES AND NOTES


1. N. Yu, F. Capasso, *Nat. Mater.* **13**, 139–150 (2014).
2. A. V. Kildishev, A. Boltasseva, V. M. Shalaev, *Science* **339**, 1232009 (2013).
3. N. Yu *et al.*, *Science* **334**, 333–337 (2011).
4. X. Ni, N. K. Emani, A. V. Kildishev, A. Boltasseva, V. M. Shalaev, *Science* **335**, 427–427 (2012).
5. A. Silva *et al.*, *Science* **343**, 160–163 (2014).
6. F. Monticone, N. M. Estakhri, A. Alù, *Phys. Rev. Lett.* **110**, 203903 (2013).
7. S. Jahani, Z. Jacob, *Nat. Nanotechnol.* **11**, 23–36 (2016).
8. D. Fattal, J. Li, Z. Peng, M. Fiorentino, R. G. Beausoleil, *Nat. Photonics* **4**, 466–470 (2010).
9. F. Aieta, M. A. Kats, P. Genevet, F. Capasso, *Science* **347**, 1342–1345 (2015).
10. M. Khorasaninejad *et al.*, *Nano Lett.* **15**, 5358–5362 (2015).
11. D. Lin, P. Fan, E. Hasman, M. L. Brongersma, *Science* **345**, 298–302 (2014).
12. Z. Bomzon, G. Biener, V. Kleiner, E. Hasman, *Opt. Lett.* **27**, 285–287 (2002).
13. M. Khorasaninejad, K. B. Crozier, *Nat. Commun.* **5**, 5386 (2014).
14. K. E. Chong *et al.*, *Nano Lett.* **15**, 5369–5374 (2015).
15. A. Arbabi, Y. Horie, A. J. Ball, M. Bagheri, A. Faraon, *Nat. Commun.* **6**, 7069 (2015).
16. C. J. Chang-Hasnain, *Semicond. Sci. Technol.* **26**, 014043 (2011).
17. Y. Yang *et al.*, *Nano Lett.* **14**, 1394–1399 (2014).
18. M. Khorasaninejad, W. Zhu, K. Crozier, *Optica* **2**, 376–382 (2015).
19. P. Spinelli, M. A. Verschuuren, A. Polman, *Nat. Commun.* **3**, 692 (2012).
20. S. Liu *et al.*, *Optica* **1**, 250–256 (2014).
21. G. Zheng *et al.*, *Nat. Nanotechnol.* **10**, 308–312 (2015).
22. E. T. Rogers *et al.*, *Nat. Mater.* **11**, 432–435 (2012).
23. S. Sun *et al.*, *Nano Lett.* **12**, 6223–6229 (2012).
24. S. Larouche, Y.-J. Tsai, T. Tyler, N. M. Jokerst, D. R. Smith, *Nat. Mater.* **11**, 450–454 (2012).
25. F. Aieta *et al.*, *Nano Lett.* **12**, 4932–4936 (2012).
26. X. Yin, Z. Ye, J. Rho, Y. Wang, X. Zhang, *Science* **339**, 1405–1407 (2013).
27. W. T. Chen *et al.*, *Nano Lett.* **14**, 225–230 (2014).
28. A. Grbic, L. Jiang, R. Merlin, *Science* **320**, 511–513 (2008).
29. M. Khorasaninejad, F. Capasso, *Nano Lett.* **15**, 6709–6715 (2015).
30. R. Merlin, *Science* **317**, 927–929 (2007).
31. R. C. Devlin, M. Khorasaninejad, W.-T. Chen, J. Oh, F. Capasso, arXiv:1603.02735 (2016).
32. A. A. High *et al.*, *Nature* **522**, 192–196 (2015).
33. M. V. Berry, *J. Mod. Opt.* **34**, 1401–1407 (1987).
34. S. Pancharatnam, *Proceedings of the Indian Academy of Sciences, Section A* (Springer, 1956), vol. 44, pp. 398–417.
35. Supplementary materials are available on *Science* Online.
36. M. Yoshida, U.S. Patent App. 13/760,681, 2013.
37. F. Aieta, P. Genevet, M. Kats, F. Capasso, *Opt. Express* **21**, 31530–31539 (2013).


## ACKNOWLEDGMENTS

This work was supported in part by the Air Force Office of Scientific Research (MURI, grant FA9550-14-1-0389), Charles Stark Draper Laboratory, Inc. (SC001-0000000959), and Thorlabs Inc. W.T.C. acknowledges postdoctoral fellowship support from the Ministry of Science and Technology, Taiwan (104-2917-I-564-058). R.C.D. is supported by a Charles Stark Draper Fellowship. A.Y.Z. thanks Harvard John A. Paulson School of Engineering and Applied Sciences and A*STAR Singapore under the National Science Scholarship scheme. Fabrication work was carried out in the Harvard Center for Nanoscale Systems, which is supported by the NSF. We thank E. Hu for the supercontinuum laser (NKT "SuperK").

## SUPPLEMENTARY MATERIALS

www.sciencemag.org/content/352/6290/1190/suppl/DC1
Materials and Methods
Figs. S1 to S10
Movie S1
References (*38*, *39*)

10 March 2016; accepted 22 April 2016
10.1126/science.aaf6644

REPORTS

WATER CHEMISTRY

# Structure and torsional dynamics of the water octamer from THz laser spectroscopy near 215 μm

**William T. S. Cole,[1]* James D. Farrell,[2]* David J. Wales,[2]† Richard J. Saykally[1]†**

**Clusters of eight water molecules play an important role in theoretical analysis of aqueous structure and dynamics but have proven to be challenging experimental targets. Here we report the high-resolution spectroscopic characterization of the water octamer. Terahertz (THz) vibration-rotation-tunneling (VRT) spectroscopy resolved 99 transitions with 1 part per million precision in a narrow range near 46.5 wave numbers, which were assigned to the $h_{16}$ octamer via detailed isotope dilution experiments. Fitting to a semi-rigid symmetric top model supports predictions of two coexisting cuboidal structures and provides precise values for the changes in their rotational constants. Comparison with theory and previous spectroscopic data provides a characterization of the two structures and the observed torsional vibration and supports the prediction that the $D_{2d}$ symmetry structure is lower in energy than the $S_4$ isomer.**

Spectroscopic study of water clusters provides accurate benchmarks for detailed characterization of the complex pairwise and many-body forces that operate in bulk water phases, which have proven difficult to adequately capture through bulk experiments or theory (*1*–*4*). The need to accomplish this goal is underscored by recurring controversies surrounding the fundamental intermolecular structure and dynamics of water (*2*, *5*, *6*). Clusters ranging from dimer through heptamer, as well as nonamer and decamer (*7*), have been studied in detail by high-precision microwave and terahertz spectroscopy, but the octamer has proven elusive (*1*, *2*, *8*–*10*). Whereas the most stable structures of smaller clusters evolve with size from quasiplanar rings to three-dimensional (3D) cages, the octamer represents the transition to cuboidal (*8*) structures formed by stacking quasiplanar four- and five-membered rings, a dominant motif in larger systems.

Accordingly, the water octamer has become a benchmark for theory, starting with the early work of Stillinger and David (*11*), Brink and Glasser (*12*), and Tsai and Jordan (*13*). Many groups have since investigated the structures, melting transitions, and hydrogen bond (HB) rearrangement dynamics of the octamer cluster (*14*–*30*). However, experimental characterization has been very challenging, with only a few successful mid-infrared (IR) spectroscopy (*31*–*34*) and crystallographic studies (*35*–*37*). The mid-IR results are particularly interesting, revealing two nonpolar low-energy structures (Fig. 1) formed by stacking of homodromic tetramer rings with the in-plane HBs directed in either the same ($S_4$ symmetry) or opposite ($D_{2d}$ symmetry) senses. Both structures possess two distinct monomer environments: single HB donor and double HB donor, with the latter responsible for the association between the two tetramer rings. These structures have subsequently been refined by theory, with several groups calculating the ground state energy difference between the $S_4$ and the $D_{2d}$ structures to be <0.1 kJ/mol (*14*–*17*, *37*). Given such a small energy difference, both structures should be present even in very low temperature environments, e.g., supersonic beams.

Here we present the results of a study of the water $h_{16}$-octamer by terahertz vibration-rotation-tunneling (VRT) spectroscopy, involving the measurement of a very low frequency torsional vibration in both low-lying isomers. Nearly 100 individual vibration-rotation transitions have been measured to parts per million (ppm) accuracy and fitted to a standard semi-rigid symmetric rotor model, producing rotational constants, which, when combined with theoretical values, characterize the structures and vibrational distortions of the cluster. The results are in good agreement with recent theoretical predictions of the HB rearrangement tunneling rates (*8*) and cluster structures.

In an earlier study, Richardson *et al.* presented VRT spectra comprising 99 weak transitions measured near 1.4 THz and assigned to the $h_{16}$-water octamer cluster on the basis of detailed isotopic dilution studies (*8*). Spectral assignment was not possible at that time. In the same study, application of the ring polymer perturbative instanton method predicted the HB rearrangement tunneling rates for the $h_{16}$-octamer. Those results indicated that even for the most energetically accessible rearrangement, the magnitude of the tunneling

[1]Department of Chemistry, University of California, Berkeley, CA 94705, USA. [2]Department of Chemistry, University of Cambridge, Cambridge CB2 1EW, UK.
*These authors contributed equally to this work. †Corresponding author. Email: saykally@berkeley.edu (R.J.S.); dw34@cam.ac.uk (D.J.W.)

splitting was <42 Hz, well below our experimental resolution (~1 MHz). Subsequently, we have employed a statistical spectral assignment algorithm, which has enabled the detailed assignment of the spectra. A least-squares fit of the transitions yielded precise values for the vibrationally induced changes in the rotational constants of both isomers, which, in combination with the earlier results of Gruenloh *et al.* (*32*, *33*), provide a good estimate of the excited state rotational constants. Harmonic normal mode analysis predicts a diamond-type vibrational mode, shown in Fig. 1, for both isomer structures.

The measurement of VRT spectra and assignment to the $h_{16}$-water octamer with the Berkeley Terahertz spectrometer is described in detail in (*1*–*3*) and in the supplementary materials. Because the 99 measured octamer transitions are confined to a very compact region (~350 MHz), it was assumed that the transitions belong to a Q branch. This is consistent with our previous THz VRT results for the similar $h_{12}$-hexamer, in which the Q branches were observed to have higher intensity than P- or R-branch transitions. To approach assignment of the very dense observed spectrum, we created a pattern recognition program to search the spectrum for transitions that displayed the energy-level pattern characteristic of the $D_{2d}$ and $S_4$ structures. These patterns are distinct in that the $D_{2d}$ equilibrium structure is an oblate symmetric rotor, whereas the $S_4$ structure is a prolate symmetric rotor, exhibiting opposite-intensity variations with the same J-quantum numbers. Using the output of this program as a starting point facilitated the assignment of 91 transitions to the $D_{2d}$ (60 transitions) and $S_4$ (31 transitions) structures. The assignment, along with the eight weak unassigned lines, is shown in Fig. 2A. Figure 2, B and C, shows a comparison between the calculated and observed experimental spectrum for a representative Q-branch progression of each symmetry. As predicted (*8*), no evidence for tunneling splittings was observed. Figure 3 shows a measured vibration-rotation absorption feature, compared with the predicted tunneling splitting. We ultimately determined that the assigned transitions belong to two distinct parallel ($\Delta K = 0$) bands. The complete collection of assigned transitions is given in tables S1 and S2.

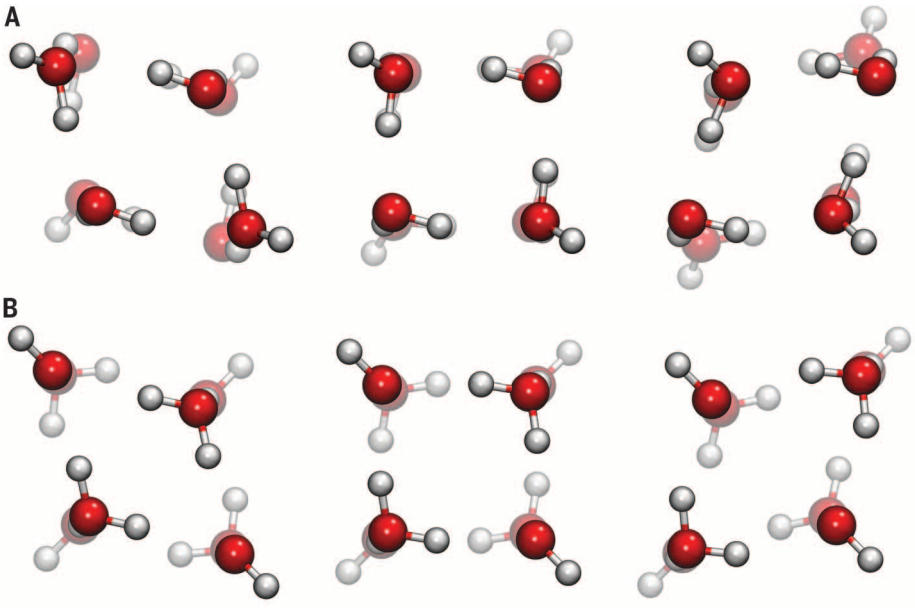


**Fig. 1. The two lowest-energy structures predicted for the water octamer, viewed along the principal axes.** Tentatively assigned low-frequency vibrational motions are also depicted. (**A**) The $S_4$ structure, viewed along the long axis (middle), pictured with displacements along the normal mode on either side. (**B**) The corresponding $D_{2d}$ structure and displacements, viewed along the short axis. The $D_{2d}$ structure is predicted to be slightly lower in energy, whereas entropy favors the $S_4$ structure (*16*).

**Table 1. Fitted constants (in MHz) for the $D_{2d}$ structure based on 60 assigned transitions.** Band origin is 46.13503 ($cm^{-1}$). Root mean square deviation of fit: 2.7 MHz.

| Constant | Value | Error |
|---|---|---|
| $\Delta B$ | 4.455 | $3.0 \times 10^{-2}$ |
| $\Delta M$ | 0.881 | $8.3 \times 10^{-3}$ |
| $\Delta D_J$ | $1.03 \times 10^{-2}$ | $9.0 \times 10^{-5}$ |
| $\Delta D_{JK}$ | $1.74 \times 10^{-2}$ | $7.9 \times 10^{-4}$ |
| $\Delta D_K$ | $-4.13 \times 10^{-4}$ | $4.5 \times 10^{-5}$ |
| Band origin | 1383093.60 | 1.6 |

**Table 2. Fitted constants (in MHz) for the $S_4$ structure based on 31 assigned transitions.** Band origin is 46.13951 ($cm^{-1}$). Root mean square deviation of fit: 2.5 MHz.

| Constant | Value | Error |
|---|---|---|
| $\Delta B$ | 2.705 | $1.3 \times 10^{-1}$ |
| $\Delta M$ | 1.960 | $9.6 \times 10^{-2}$ |
| $\Delta D_J$ | $-1.58 \times 10^{-3}$ | $3.3 \times 10^{-4}$ |
| $\Delta D_{JK}$ | $-1.40 \times 10^{-2}$ | $3.3 \times 10^{-3}$ |
| $\Delta D_K$ | $4.16 \times 10^{-3}$ | $8.6 \times 10^{-4}$ |
| Band origin | 1383227.90 | $5.5 \times 10^{-1}$ |

After assignment, the transitions were fitted to a standard, semi-rigid rotor energy-level expression (Eq. 1):

$$E(J,K) = \nu + \Delta B \times J(J+1) + \Delta M \times K^2 - \Delta D_J \times J^2(J+1)^2 - \Delta D_{JK} \times J(J+1)K^2 - \Delta D_K \times K^4 \quad (1)$$

Here ν is the band origin, $B$ is the perpendicular rotational constant, and the $D$ terms are the standard centrifugal distortion constants. The band origins are defined with respect to the absolute ground state of the respective cluster structures. All differences are defined as excited state minus ground state. The term $\Delta M$ is

$$\Delta M = (A' - B') - (A'' - B'') \text{ for the } S_4 \text{ octamer}$$

$$\Delta M = (B'' - C'') - (B' - C') \text{ for the } D_{2d} \text{ octamer}$$

Here ν is the band origin, $B$ is the perpendicular rotational constant, and the $D$ terms are the standard centrifugal distortion constants. The band origins are defined with respect to the absolute ground state of the respective cluster structures. All differences are defined as excited state minus ground state. The term $\Delta M$ is

$$\Delta M = (A' - B') - (A'' - B'') \text{ for the } S_4 \text{ octamer}$$

$$\Delta M = (B'' - C'') - (B' - C') \text{ for the } D_{2d} \text{ octamer}$$

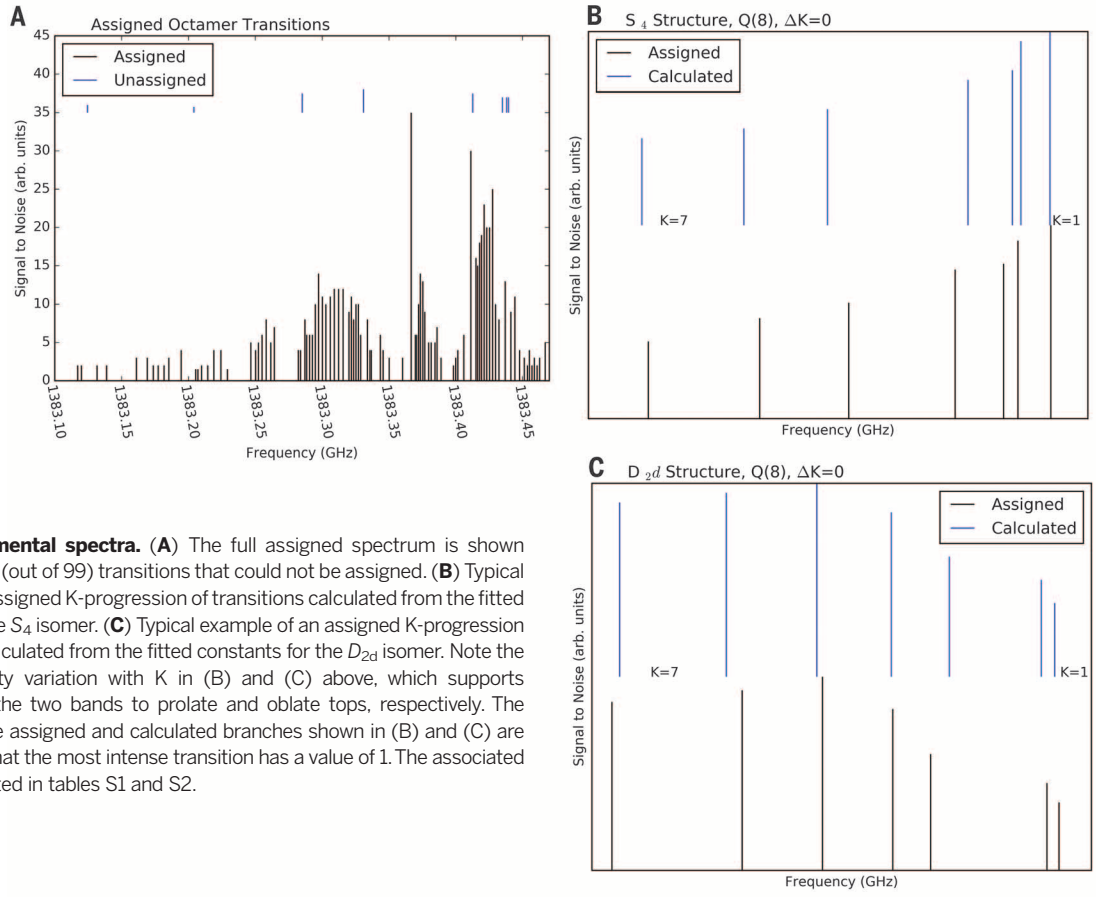


**Fig. 2. Experimental spectra.** (**A**) The full assigned spectrum is shown along with the 8 (out of 99) transitions that could not be assigned. (**B**) Typical example of an assigned K-progression of transitions calculated from the fitted constants for the $S_4$ isomer. (**C**) Typical example of an assigned K-progression of transitions calculated from the fitted constants for the $D_{2d}$ isomer. Note the opposite-intensity variation with K in (B) and (C) above, which supports assignment of the two bands to prolate and oblate tops, respectively. The intensities of the assigned and calculated branches shown in (B) and (C) are normalized so that the most intense transition has a value of 1. The associated data are presented in tables S1 and S2.

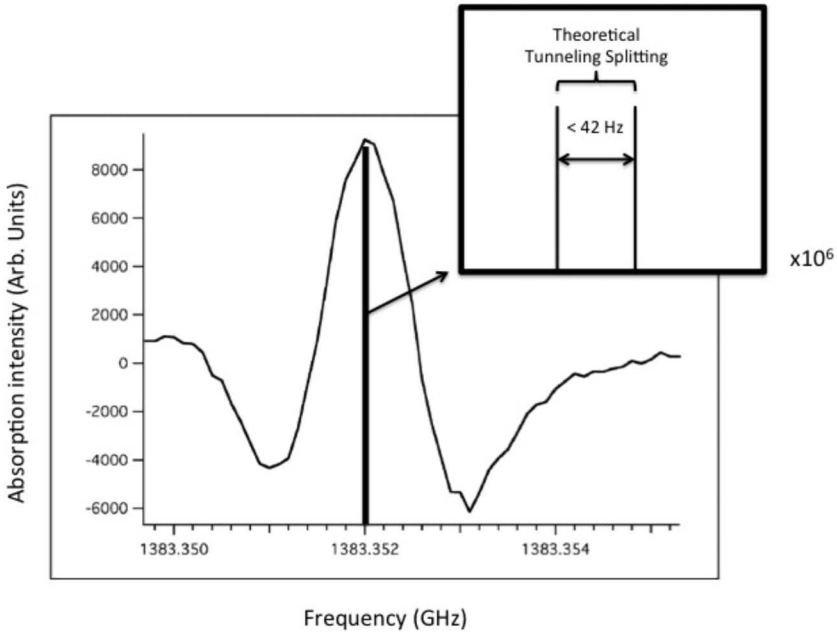


**Fig. 3. A measured absorption transition showing the characteristic second derivative line shape observed.** The full width at half-maximum linewidths are ~1 MHz. Tunneling splittings predicted in (*8*) are well below the experimental resolution, which is determined by the residual Doppler width in the planar supersonic expansion.

A and C represent the two remaining rotational constants, and primed values refer to excited state terms, whereas the double-primed values are those of the ground state. The difference in the $\Delta M$ terms reflects the two octamer structures being different types of symmetric rotors, as previously noted.

A least-squares fit of the 91 assigned transitions to Eq. 1 yielded root mean square deviations of 2.7 MHz ($D_{2d}$) and 2.5 MHz ($S_4$), respectively. Tables 1 and 2 present the fitted constants of both octamer structures for the ground and excited states, along with the 1σ errors. Correlation matrices for the fits are given in figs. S1 and S2. Although a simple symmetric top rigid rotor energy expression produced a good fit of the assigned data, it is well known that water clusters are actually highly nonrigid complexes and as such may violate simple selection rules because the projection of rotational angular momentum along the symmetry axis (quantum number, K) is not rigorously conserved (*2*, *38*).

Although spectroscopic determination of structural parameters is not possible without R- or P-branch assignments, the detailed isotope dilution results previously presented in (*8*) and the absence of any asymmetry splittings unambiguously identified the spectral carrier as the $h_{16}$-water octamer.

The observation of two distinct bands (at 46.13503 and 46.13951 $cm^{-1}$) can be rationalized in two ways. Either the bands could originate from two different vibrational modes of a single octamer structure, or each could belong to a similar vibration from separate octamer isomers. We argue that the second option is more likely. Two experimental observations support this conclusion. First, the two bands have opposite-intensity patterns, one displaying higher K components with lower intensity and the other higher K components with higher intensity, as evident in Fig. 2, B and C. These observations are consistent with the ground state energy-level diagrams of prolate and oblate symmetric tops, respectively. We have neglected vibrationally induced dipole changes here, as the transitions within a Q branch can reasonably be assumed not to differ appreciably in that regard. Second, the vibrational changes in rotational constants of the two bands are markedly similar, indicating that the corresponding motions are nearly identical. Moreover, even in molecules of this size, it is unlikely that two modes would exist in such extreme proximity (less than 0.005 $cm^{-1}$) as observed herein. On the basis of these considerations, we are confident in assigning the two bands to different water octamer isomers, one an oblate symmetric top and the other a prolate top.

Because the supersonic expansion cools the clusters to about 4 K, we are confident that the two structures are the $D_{2d}$ and $S_4$ isomers, because they are consistently predicted to be particularly close in energy (*14*, *17*, *27*, *30*, *32*) and to have prolate ($S_4$) and oblate ($D_{2d}$) symmetric rotor eigenstates. On this basis, we assign the two observed bands to the $S_4$ or $D_{2d}$ water octamer isomers.

The group comprising the energetically accessible permutation-inversion operations for the water octamer (i.e., operations that do not break a covalent bond) contains on the order of $8! \times 2^8 \times 2 = \sim 10^8$ elements. As for previous water clusters (*1*–*3*, *25*), the water octamer is expected to display a high degree of nonrigidity. Assuming a rigid system enables us to exploit the corresponding point groups; however, this simplification may fail if the system is substantially nonrigid. A symmetric rotor energy-level expression is thus an approximation of the true energy-level structure of the complex. As with other water clusters, nonrigidity could lead to tunneling splittings of the simple symmetric top rigid rotor energy levels. Although we did not observe any tunneling in the spectra reported herein (in agreement with predictions) (*8*), the system still displays substantial nonrigidity in the form of low-frequency torsional vibrations and relaxed selection rules. A direct consequence of this nonrigidity is encountered in the description of the vibrational mode observed herein.

The observed transitions belong to parallel bands, implying a change in the dipole moment along the principal rotation axis. This result requires the observed vibration to have B symmetry in the case of the $S_4$ structure and $B_2$ symmetry for the $D_{2d}$ competitor. A normal-mode analysis with the MB-pol potential (*4*, *39*, *40*) reveals that the lowest-frequency $B_2$ vibration corresponds to the pattern in Fig. 1B, where the tetramers in the perpendicular plane distort to diamond geometries (see supplementary materials for methodological details and harmonic frequencies). The harmonic frequency of this mode is 74.8 $cm^{-1}$. The next lowest $B_2$ mode occurs at 204.1 $cm^{-1}$, involving the antisymmetric compression and expansion of the perpendicular faces. It is unlikely that these modes would reorder upon inclusion of anharmonic effects.

Given that both octamer structures display similar changes in rotational constants and noting the close proximity of the two bands, it is reasonable to expect that this vibrational motion is similar in the $D_{2d}$ and $S_4$ isomers. The two lowest B modes of the $S_4$ structure occur at 69.9 and 76.9 $cm^{-1}$, the second of which is most similar in frequency to the mode assigned to the $D_{2d}$ vibration and describes an almost identical displacement (Fig. 1A).

We stress that this description of the vibrational motion is but a starting point for future work. Previous studies of water clusters (*1*–*3*, *38*, *41*) have shown that nonrigidity results in vibrational motions that deviate appreciably from simple harmonic or rigid rotor approximations. Detailed quantitative analysis of the intermolecular vibrations in the octamer will clearly require further experiments and calculations.

Given the complexity of the nonrigid octamer structures, spectroscopically accurate calculations for the vibrational modes present a major challenge. Furthermore, a simple analysis of the energy landscape using TIPXP water potentials ($X = 3$ to 5) suggests that the number of minima may increase rapidly in the presence of an electric field (*23*). Shields and co-workers (*17*, *27*) report the lowest anharmonically corrected ab initio intermolecular vibrational frequencies for the octamer as 57.2 ($D_{2d}$) and 54.7 ($S_4$) wave numbers, considerably higher than the experimental values near 46.1 $cm^{-1}$. Clearly, further theoretical advances are necessary to compute such cluster properties reliably, noting that much progress in this regard has recently been achieved for the water hexamer (*41*).

Finally, we report evidence in support of calculations showing that the $D_{2d}$ structure is the lowest in energy (*14*, *23*, *27*, *29*). If we assume that the transition dipole moment is similar for the competing cuboids, we can use the number and intensities of the observed transitions to infer the relative energetics. For the $D_{2d}$ structure, we observe J values from 2 to 17, with some of the higher J subbands lacking some K value components. For the $S_4$ structure, we observe J values of only 5 to 10, and again, the higher J subbands are missing some K-value transitions. From this evidence, we infer that the $D_{2d}$ structure is the lowest in energy.

## REFERENCES AND NOTES


1. K. Liu, J. D. Cruzan, R. J. Saykally, *Science* **271**, 929–933 (1996).
2. F. N. Keutsch, R. J. Saykally, *Proc. Natl. Acad. Sci. U.S.A.* **98**, 10533–10540 (2001).
3. A. Mukhopadhyay, W. T. S. Cole, R. J. Saykally, *Chem. Phys. Lett.* **633**, 13–26 (2015).
4. V. Babin, C. Leforestier, F. Paesani, *J. Chem. Theory Comput.* **9**, 5395–5403 (2013).
5. R. S. Fellers, C. Leforestier, L. B. Braly, M. G. Brown, R. J. Saykally, *Science* **284**, 945–948 (1999).
6. Y. Wang, V. Babin, J. M. Bowman, F. Paesani, *J. Am. Chem. Soc.* **134**, 11116–11119 (2012).
7. C. Pérez *et al.*, *Angew. Chem. Int. Ed. Engl.* **53**, 14368–14372 (2014).
8. J. O. Richardson *et al.*, *J. Phys. Chem. A* **117**, 6960–6966 (2013).
9. C. Pérez *et al.*, *Chem. Phys. Lett.* **571**, 1–15 (2013).
10. C. Pérez *et al.*, *Science* **336**, 897–901 (2012).
11. F. Stillinger, C. W. David, *J. Chem. Phys.* **73**, 3384 (1980).
12. G. Brink, L. Glasser, *J. Phys. Chem.* **88**, 3412–3414 (1984).
13. C. J. Tsai, K. D. Jordan, *J. Chem. Phys.* **95**, 3850 (1991).
14. S. S. Xantheas, E. Aprà, *J. Chem. Phys.* **120**, 823–828 (2004).
15. M. B. Day, K. N. Kirschner, G. C. Shields, *Int. J. Quantum Chem.* **102**, 565–572 (2005).
16. R. M. Shields, B. Temelso, K. A. Archer, T. E. Morrell, G. C. Shields, *J. Phys. Chem. A* **114**, 11725–11737 (2010).
17. B. Temelso, G. C. Shields, *J. Chem. Theory Comput.* **7**, 2804–2817 (2011).
18. E. Asare, A. R. Musah, E. Curotto, D. L. Freeman, J. D. Doll, *J. Chem. Phys.* **131**, 184508 (2009).
19. J. Hernández-Rojas, B. S. González, T. James, D. J. Wales, *J. Chem. Phys.* **125**, 224302 (2006).
20. P. Nigra, M. A. Carignano, S. Kais, *J. Chem. Phys.* **115**, 2621 (2001).
21. Y. Sun, E. Gao, D. Wei, *Inorg. Chem. Commun.* **10**, 467–470 (2007).
22. D. J. Wales, I. Ohmine, *J. Chem. Phys.* **98**, 7245 (1993).
23. T. James, D. J. Wales, J. Hernández Rojas, *J. Chem. Phys.* **126**, 054506 (2007).
24. A. Tharrington, K. D. Jordan, *J. Phys. Chem. A* **107**, 7380–7389 (2003).
25. D. J. Wales, I. Ohmine, *J. Chem. Phys.* **98**, 7257 (1993).
26. T. Miyake, M. Aida, *Chem. Phys. Lett.* **427**, 215–220 (2006).
27. B. Temelso, K. A. Archer, G. C. Shields, *J. Phys. Chem. A* **115**, 12034–12046 (2011).
28. J. Gelman-Constantin, M. A. Carignano, I. Szleifer, E. J. Marceca, H. R. Corti, *J. Chem. Phys.* **133**, 024506 (2010).
29. S. Maeda, K. Ohno, *J. Phys. Chem. A* **111**, 4527–4534 (2007).
30. E. Miliordos, S. S. Xantheas, *J. Chem. Phys.* **142**, 234303 (2015).
31. U. Buck, I. Ettischer, M. Melzer, V. Buch, J. Sadlej, *Phys. Rev. Lett.* **80**, 2578–2581 (1998).
32. C. J. Gruenloh *et al.*, *Science* **276**, 1678–1681 (1997).
33. C. J. Gruenloh *et al.*, *J. Chem. Phys.* **109**, 6601 (1998).
34. B. P. Suitte, S. D. Belair, J. S. Francisco, *Phys. Rev. A* **71**, 043204 (2005).
35. W. B. Blanton *et al.*, *J. Am. Chem. Soc.* **121**, 3551 (1999).
36. H.-J. Hao, D. Sun, F.-J. Liu, R.-B. Huang, L.-S. Zheng, *Cryst. Growth Des.* **11**, 5475–5482 (2011).
37. T. K. Prasad, M. V. Rajasekharan, *Cryst. Growth Des.* **6**, 488–491 (2006).
38. J. D. Cruzan *et al.*, *Science* **271**, 59–62 (1996).
39. V. Babin, G. R. Medders, F. Paesani, *J. Chem. Theory Comput.* **10**, 1599–1607 (2014).
40. G. R. Medders, V. Babin, F. Paesani, *J. Chem. Theory Comput.* **10**, 2906–2910 (2014).
41. J. O. Richardson *et al.*, *Science* **351**, 1310–1313 (2016).


## ACKNOWLEDGMENTS


The Berkeley Terahertz project is supported by Chemical Structure, Dynamics, and Mechanisms–A Division of the National Science Foundation under grant no. 1300723. J.D.F. gratefully acknowledges A. Thom and D. Chakraborty for stimulating discussions. We thank the referees for thoughtful discussion during review. For details of the pattern recognition methodology, contact the authors or visit www.cchem.berkeley.edu/rjsgrp/.


## SUPPLEMENTARY MATERIALS

www.sciencemag.org/content/352/6290/1194/suppl/DC1
Materials and Methods
Figs. S1 and S2
Tables S1 to S5
References (*42*–*46*)


12 November 2015; accepted 2 May 2016
10.1126/science.aad8625

**Structure and torsional dynamics of the water octamer from THz laser spectroscopy near 215 μm**

William T. S. Cole, James D. Farrell, David J. Wales and Richard J. Saykally (June 2, 2016)

*Science* **352** (6290), 1194-1197. [doi: 10.1126/science.aad8625]

Editor's Summary

**A close-up look at eight water molecules**

A raindrop may look small, but it contains far too much water to model with the highest chemical precision. Theorists rely on studies of clusters with just a few molecules to enhance their understanding of the quantum-mechanical forces at play in the liquid. Cole *et al.* now report a high-resolution spectrum in the terahertz regime of the eight-membered cluster. By resolving 99 absorption lines associated with a collective torsional mode, the authors distinguish prolate and oblate isomers that are very similar in energy.

*Science*, this issue p. 1194



*Science* (print ISSN 0036-8075; online ISSN 1095-9203) is published weekly, except the last week in December, by the American Association for the Advancement of Science, 1200 New York Avenue NW, Washington, DC 20005. 